Geochemistry of the Komatiite–Tholeiite Rock Association in the Vedlozero–Segozero Archean Greenstone Belt, Central Karelia

S. A. Svetov*, A. I. Svetova*, and H. Huhma**

* Institute of Geology, Karelian Scientific Center, Russian Academy of Sciences,
Pushkinskaya ul. 11, Petrozavodsk, 185610 Karelia, Russia
e-mail: ssvetov@post.krc.karelia.ru
** Geological Survey of Finland, GSF FIN-02150, Betonimiehenkuja 4, Espoo, Finland
Received May 12, 1999

Abstract—High-Mg volcanics of the komatiite and tholeiite types are widespread in the greenstone belts of Karelia. Their geochemistry and isotopic features were examined using representative successions of the Late Archean Vedlozero–Segozero greenstone belt in central Karelia. The overall thickness of the rocks of the komatiite–tholeiite associations ranges from 2.8 (at Koikary) to 1.5–1.0 km (at Palasel'ga and Sovdozero). The sequences are made up of massive, pillow, and variolitic differentiated lava flows with thin beds of tuff material. The contents of pyroclastic facies do not exceed 3–5% of the overall rock volumes. Tholeiitic basalts overlay komatiites or alternate with them. The successions are dominated by pyroxenitic and basaltic komatiites and Mg-tholeiites. The Sovdozero structure is volumetrically dominated by peridotitic komatiites. The rocks are altered to the greenschist and epidote amphibolite metamorphic facies. Based on the $CaO/Al_2O_3 \approx 0.8$ and $Al_2O_3/TiO_2 \approx 22$ ratios and on the HREE patterns $(Gd/Yb)_n = 0.99-1.17$, the komatiites are classed with the Al-undepleted type. Compared with the komatiitic lavas, compositionally analogous tuffs have lower concentrations of Al_2O_3 (<8%), are higher in CaO (7–9%), and lower in alkalis. The tholeiites of the belt are geochemically close to basaltic komatiites. Based on experimental results, we calculated the *P–T* conditions of komatiitic magma generation. The melts were produced during the process of a partial (45–60%) melting of a mantle source with the origin of *Ol + Opx* residue at depths of 210–240 km, under pressures of 6–7 GPa, and at temperatures of 1780–1845°C in the source (which is 220–280°C higher than the model temperature values in the mantle at 2.9–3.1 Ga). The maximum temperature of the melt during its eruption was as high as 1560–1615°C. The Sm–Nd age of the komatiite association is 2893 ± 110 Ma ($\varepsilon_{Nd} = +1.2$, MSWD = 7) for the Palasel'ga structure and 2944 ± 170 Ma ($\varepsilon_{Nd} = +1.7$, MSWD = 2) for the Koikary structure. The high-Mg volcanic rocks of the Vedlozero–Segozero greenstone belt were produced at 2921 ± 55 Ma ($\varepsilon_{Nd} = +1.5$, MSWD = 5) which is consistent with U–Pb ages of acid volcanics.

INTRODUCTION

Volcanic rocks of komatiite–tholeiitic associations are inherent components of rock sequences in Archean greenstone belts in the Baltic Shield. They serve as an important source of information about the conditions of mantle magma genesis. The sequences of these rocks were thoroughly examined during the geological, petrological, and geochemical studies of high-Mg assemblages in Kuhmo–Suomussalmi and Ilomantsi greenstone belts in eastern Finland [1, 2], Gimol'sko–Kostomuksha and Sumozero–Kenozero in Karelia [3–5], and Kolmozero–Voron'ya in the Kola Peninsula [6, 7].

Our research was focused on the geochemistry and isotopic features of the high-Mg volcanics from the most representative sections of the Vedlozero–Segozero greenstone belt, which is typical of central Karelia. This paper presents our newly obtained data, which make it possible to significantly clarify the processes of magma generation, as well as the differentiation and crystallization of Late Archean komatiite–tholeiite associations.

GEOLOGY

The Vedlozero–Segozero greenstone belt in the central part of the Karelian province of the Baltic Shield extends in a roughly south–north direction between Vedlozero and Segozero lakes over a distance of approximately 300 km and has a width of 50–60 km (Fig. 1).

Within the belt, Upper Archean volcano–sedimentary rocks are preserved in a series of local structures (Khautavaara, Koikary, Palasel'ga, Semch, and Sovdozero), which are expressed, in map view, as subparallel zones separated by granite-gneiss microblocks. A characteristic feature of the belt is the wide occurrence of both komatiite–tholeiite associations and calc–alkaline magmas: intermediate–acid volcanics that com-
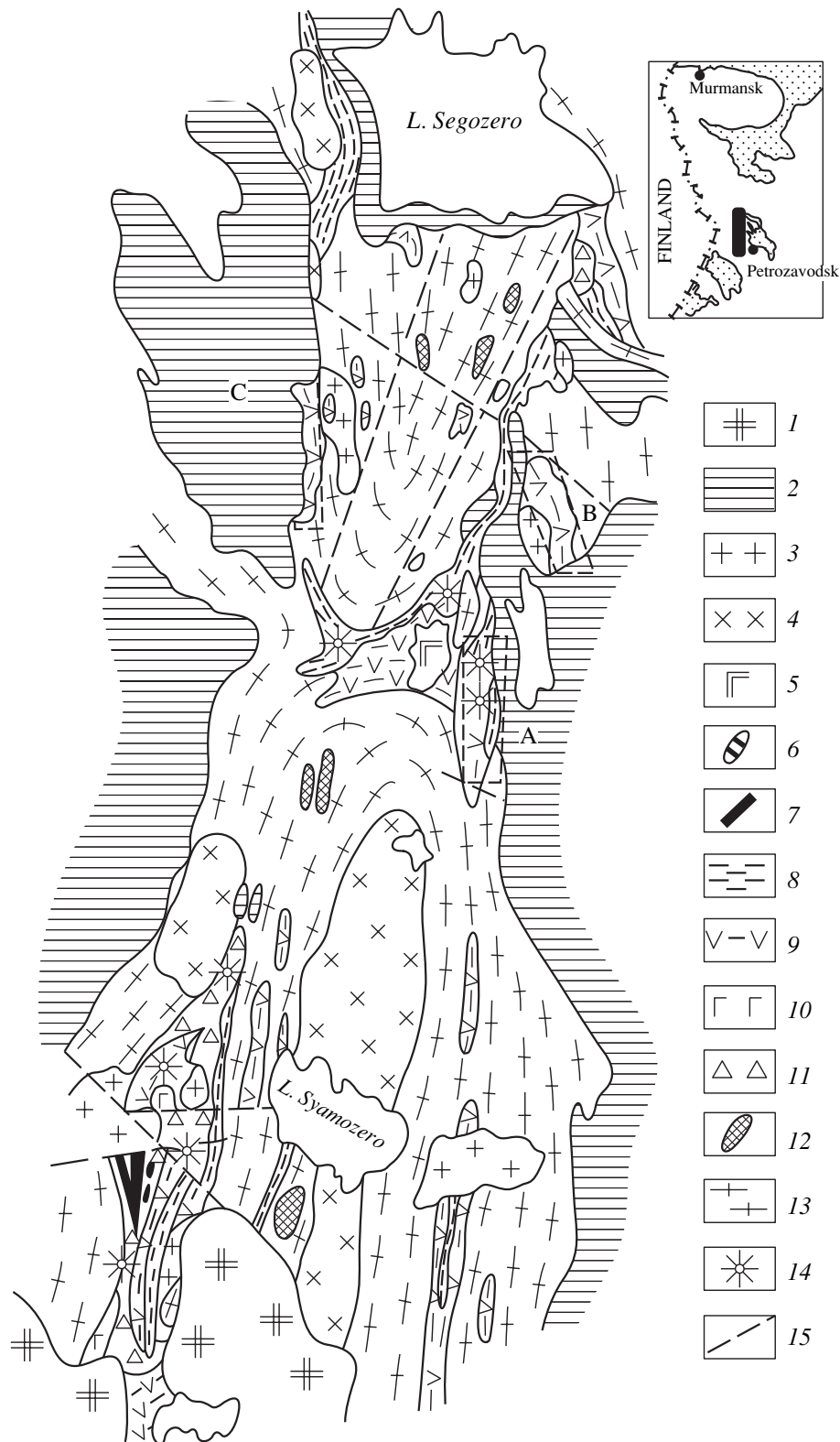
Fig. 1. Schematic geological map of the Vedlozero–Segozero greenstone belt.
Structures: A—Koikary, B—Palasel'ga, C—Sovdozero. (*1*) Rapakivi granite, (*2*) Proterozoic rocks; Lopian: (*3*) plagioclase–microcline granite, (*4*) diorite and granodiorite, (*5*) gabbrodiorite, (*6*) gabbronorite, (*7*) mafic and ultramafic rocks, (*8*) acid volcanic and sedimentary rocks, (*9*) komatiite and tholeiite lavas and tuffs, (*10*) high-Mg gabbro, (*11*) dacitic andesite, (*12*) amphibolite, (*13*) gneiss-granite and migmatite-granite, (*14*) paleovolcanic edifices, (*15*) faults.

pose volcanic edifices of the central type, whose relics were described in some of the structures [8, 9]. The reconstructed thicknesses of the komatiite–tholeiite volcanic piles range from 2.8 (Koikary–Semch) to 1.5–1.0 km (Palasel'ga and Sovdozero). The maximum integral thickness of the Archean rocks attains 6 km. In the aforementioned structures, mafic volcanics compose compact outcrops, whose areas are as follows: 2.12 km^2 at Koikary, 28.6 km^2 at Semch, 24.7 km^2 at Palasel'ga, and 1.85 km^2 at Sovdozero. The rocks are massive, pillow, and variolitic differentiated lavas with tuff beds. The amounts of pyroclastics do not exceed 3–5% of the overall rock volume. Tholeiites rest on komatiites in the Koikary structure and alternate with komatiites in the Palasel'ga and Sovdozero structures. The comagmatic intrusive associations are gabbro-diabase and ultramafite bodies.

The komatiite–tholeiite associations discussed in this paper are dated at 2900–3100 Ma. The previously obtained age of the underlying acid volcanics of the Ignoil'skii volcanic stock in the Khautavaara structure and a dacite flow is 2995 ± 20 Ma [10], and the dacite dikes and subvolcanic bodies crosscutting the komatiite–tholeiite succession of the Koikary structure were dated at 2935 ± 15 and 2860 ± 15 Ma [11, 12].

METAMORPHISM, PETROGRAPHY, AND FACIES VARIABILITY OF ROCKS

The rocks of the komatiite–tholeiite association underwent regional metamorphism of the andalusite–sillimanite type under greenschist- and epidote-amphibolite-facies conditions [13] during the Rebolian folding phase [4]. As a consequence of metamorphism, the primary magmatic minerals were fully replaced by secondary assemblages of actinolitic hornblende, anthophyllite, tremolite, serpentine, chlorite, talc, carbonate, epidote, magnetite, plagioclase, and quartz. At the same time, the rocks often contain relics of primary magmatic textures (hypocrystalline, ophitic, cumulative, and spinifex) and structural features that allow the reliable identification of the facies affiliation of the volcanic rocks. The examined geologic sequences are dominated by the lava facies. The peridotitic, pyroxenitic, and basaltic komatiites compose massive, pillow, and brecciated lava flows or, more rarely, have a differentiated inner structure. Breccia lavas can be observed in the Sovdozero structure. In the Koikary and Palasel'ga structures, groups of differentiated flows from 0.4 to 8 m thick were described. They consist of an olivine cumulate zone, spinifex textures, and breccia. The pyroxene komatiites of the Koikary structure are usually variolitic lavas. The pyroclastic rocks are tuffs with variable grain sizes: agglomerate, lapilli, and psammitic. The piles of tholeiitic basalts are dominated by pillow and massive lavas with lapilli and psammitic tuffs [14].

ANALYTICAL TECHNIQUES

For our geochemical and isotopic study, we selected samples of different facies varieties of weakly metamorphosed high-Mg volcanic and intrusive analogues from the same stratigraphic level of the Koikary, Palasel'ga, and Sovdozero structures. After petrographic examination, we discarded samples with clearly pronounced metasomatic alterations. The Sm–Nd analysis was carried out on samples with preserved relics of volcanic textures (spinifex, ophitic, and cumulative) and the weakest metamorphic transformations.

The geochemical analysis of the samples for major and trace elements, REE, and isotopes was conduced at laboratories of the Geological Survey of Finland in Espoo. The concentrations of major components, Cr, Ni, Sc, V, Cu, Pb, Zn, Bi, Mo, S, As, Rb, Ba, Sr, Ga, Nb, Zr, Y, Th, and U were determined by X-ray fluorescent analysis on a Philips PW1480 sequential X-ray spectrometric system. The errors were <2% for elements with concentrations >0.5 wt %, 5% for elements with concentrations <30 ppm, and 3% for elements with concentrations >30 ppm. REE were analyzed by ICP-MS accurate to not worse than 3%. The samples were chemically prepared for Sm–Nd analysis in compliance with the method proposed by Peltonen *et al.* [15]. The analyses were conducted by H. Huhmo on a VG sector 54 mass spectrometer. The accuracy of the $^{147}Sm/^{144}Nd$ measurements was 0.4%. The $^{143}Nd/^{144}Nd$ ratio was normalized to $^{146}Nd/^{144}Nd = 0.7219$. The measured $^{143}Nd/^{144}Nd$ value of the La Jolla standard was $0.511851 ± 6$ ($n = 15$).

We also present data from [14], which were obtained by X-ray fluorescence techniques (VRA-33) at the analytical laboratory of the Institute of Geology, Karelian Scientific Center, Russian Academy of Sciences, Petrozavodsk, and were used in constructing the classification plots.

GEOCHEMICAL CHARACTERIZATION OF THE ASSOCIATIONS

The high-Mg volcanics of the Vedlozero–Segozero greenstone belt display a widely varying chemical composition. Using an Al_2O_3–MgO–($FeO_{tot} + TiO_2$), cation %, diagram of Jensen [16], we distinguished peridotitic, pyroxenitic, and basaltic komatiites and high-Mg tholeiitic basalts. The MgO concentration of the komatiites varies from 9.4 (in basaltic komatiites) to 32% (cumulative peridotitic komatiites), and TiO_2 varies from 0.2 to 0.7% (Fig. 2; Tables 1, 2, 3). The rocks most widely occurring within the belt are basaltic komatiites (9% < MgO < 20%) and high-Mg tholeiitic basalts (8% < MgO < 15%), which are widespread in the Koikary and Palasel'ga structures. Peridotitic komatiites and their cumulative analogues (komatiitic dunites)

$(24\% < MgO < 37\%)$ are predominant only in the Sovdozero structure.

The komatiites were determined to have the following values of the indicator petrogenetic ratios: $CaO/Al_2O_3 < 1$ (Koikary 0.80 ± 0.49; Palasel'ga 0.82 ± 0.18; Sovdozero 0.86 ± 0.18), $17 < Al_2O_3/TiO_2 < 30$ (Koikary 20.20 ± 3.95; Palasel'ga 27.16 ± 3.73; Sovdozero 19.79 ± 1.35), and Zr/Y close to 2.5 (Koikary 2.63 ± 0.34; Palasel'ga 2.39 ± 0.36; Sovdozero 2.62 ± 0.67). These values, which are close to the chondritic values, led us to classify the komatiites of the Vedlozero–Segozero greenstone belt with Munro Al-undepleted type, which was first distinguished and described by Arndt and Lesher [17]. The most differentiated compositions were identified among the variolitic lavas of pyroxenitic komatiites in the Koikary structure. The composition of the varioles corresponds to low-K dacitic andesite (up to 67.61% SiO_2 and 5–8% MgO), and that of the matrix is approximated by pyroxenitic komatiite (50.9% SiO_2 and 18.9% MgO). The pyroxenitic komatiite pillow lavas show geochemical zoning, which is expressed in variations in the MgO concentration from 15–22% in the chill zone to 9–12% in the cores of pillows.

In the Jensen classification diagram [16] (Fig. 2), the tholeiitic basalts fall into the field of high-Mg or, more rarely, high-Fe tholeiites (the latter are represented by single samples from the Palasel'ga and Sovdozero structures). Some data points of the volcanics are plotted on the boundary line between the fields for high-Fe and high-Mg tholeiites. In terms of the concentrations of major elements, the tholeiitic basalts and komatiites are related by a gradual transition, which hinders their distinguishing from basaltic komatiites.

The tholeiitic basalts have the following geochemical characteristics: $TiO_2 = 0.6$–1.0% (with a maximum of 1.7%), MgO = 5–9% (with a maximum of 12%), and the CaO/Al_2O_3 ratio of <1 (Koikary 0.60 ± 0.05; Palasel'ga 0.87 ± 0.38; Sovdozero 0.73 ± 0.08), $10 < Al_2O_3/TiO_2 < 23$ (Koikary 22.08 ± 1.42; Palasel'ga 13.42 ± 4.90; Sovdozero 17.17 ± 4.56), and Zr/Y close to 2.5 (Koikary 2.49 ± 0.26; Palasel'ga 2.86 ± 0.45; Sovdozero 2.35 ± 0.31), which approach the analogous values for basaltic komatiites.

The komatiitic tuffs have major-element concentrations close to those of the lavas but are lower in Al_2O_3 (<8%), higher in CaO (7–11%), and lower in alkalis (NaO < 0.5%, $K_2O < 0.04\%$). The intrusive rocks are serpentinite and gabbro, which are cogenetic with, respectively, komatiites and tholeiitic basalts.

There is a broad range of Ni and Cr concentrations in the volcanics of the komatiite–tholeiite association. The maximum concentrations of Ni (2130 ppm) and Cr (7000 ppm) were determined in the peridotitic komatiites of the Sovdozero structure. With a decrease in the Mg# of the rocks, their Ni and Cr concentrations gradually decrease: Ni to 100–1000 ppm, Cr to 500–2000 ppm
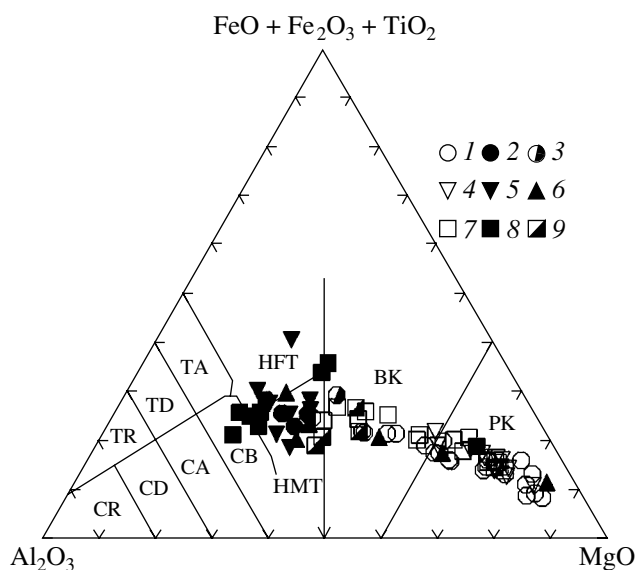
Fig. 2. Al_2O_3–MgO–(FeO + Fe_2O_3)–TiO_2 (cation %) plot [16] for rocks of the komatiite–tholeiite association of the Vedlozero–Segozero greenstone belt.

Tholeiitic series: TR—rhyolite, TD—dacite, TA—andesite; calc–alkaline series: CR—rhyolite, CD—dacite, CA—andesite, CB—basalt; HFT—high-Fe tholeiite, HMT—high-Mg tholeiite, BK—basaltic komatiite, PK—peridotitic and pyroxenitic komatiite.

Koikary structure: (1) komatiite, (2) tholeiitic basalt, (3) intrusive rocks; Sovdozero structure: (4) komatiite, (5) tholeiitic basalt, (6) intrusive rocks; Palasel'ga structure: (7) komatiite, (8) tholeiitic basalt, (9) intrusive rocks.

in the pyroxenitic komatiites; Ni to 80–200 ppm Cr to 400–1000 ppm in the basaltic komatiites; and Ni to 30−100 ppm Cr to 50–400 ppm in the tholeiitic basalts.

The distribution of Al_2O_3, TiO_2, Y, and Zr versus MgO (Fig. 3) is close to the linear trends caused by olivine fractionation (lines of *Ol* control). At the same time, the volcanics show a few trends that intersect the MgO axis at 46–50 and 35–40%, which can be explained by the involvement of a series of parental melts.

Using the values at which the olivine control lines intersect the MgO axis, we calculated the MgO concentrations of olivine in equilibrium with the parental melt [17]. Assuming that the Fe^{3+} concentration of the melt did not exceed 10% and using the partition coefficient $Kd_{(Ol–Liq)/(Mg–Fe)} = 0.3 \pm 0.03$ [18], we deduced that the parental melts have Mg# of 22–26% and 14–16%, which is lower than that of the chill zones in peridotitic komatiite flows at Koikary (27.82%), Palasel'ga (28.39%), and Sovdozero (29.44%) [14].

The volcanic rocks are characterized by the unfractionated HREE patterns and variable LREE patterns (Table 4). In the Koikary structure, the rocks of the komatiite–tholeiite association are characterized by

Table 1. Composition (wt %, ppm) of rocks of the komatiite--tholeiite association from the Koikary structure

Component	40-51	95-1	40-1	2-3	40-50	41-1	5480	350-8a	350-1	350-32	350-64	2-2	94-1	2-1
SiO_2	46.32	44.22	49.66	45.22	40.99	38.84	36.56	42.78	47.80	42.10	41.78	44.42	46.81	38.96
TiO_2	0.23	0.20	0.22	0.34	0.15	0.30	0.23	0.36	0.29	0.37	0.39	0.51	0.16	0.63
Al_2O_3	4.58	3.16	3.37	7.35	3.58	4.01	4.57	9.22	6.12	8.69	10.22	8.85	2.82	9.56
Fe_2O_3	2.49	4.81	2.91	3.16	2.43	3.51	1.82	1.40	2.12	2.63	1.50	1.66	2.61	2.07
FeO	3.30	4.31	2.60	6.61	3.44	3.68	5.56	8.91	6.82	10.20	9.91	8.05	6.29	8.90
MnO	0.08	0.14	0.09	0.17	0.13	0.12	0.36	0.16	0.11	0.16	0.20	0.19	0.12	0.20
MgO	29.73	29.96	30.56	27.82	28.69	28.76	23.79	23.34	24.49	22.11	22.48	22.78	23.62	19.43
CaO	2.16	1.12	1.26	0.56	5.19	5.05	9.81	6.52	6.31	6.58	5.46	6.73	6.32	10.50
Na_2O	0.03	0.02	0.02	0.01	0.03	0.01	0.02	0.08	0.04	0.28	0.13	0.05	0.02	0.32
K_2O	0.01	0.01	0.01	0.01	0.01	0.01	0.02	0.02	0.01	0.02	0.02	0.01	0.01	0.06
P_2O_5	0.05				0.03		0.05	0.05	0.04	0.04	0.05			
H_2O	0.09	0.20	0.10	0.10	0.12	0.07	0.09	0.19	0.21	0.36	0.22	0.42	0.11	0.16
LOI	10.52	11.53	9.09	8.18	13.46	14.41	16.54	6.38	4.99	6.39	6.83	5.90	10.40	9.36
Total	99.59	99.68	99.89	99.53	98.25	99.77	99.42	99.41	99.35	99.93	99.19	99.57	99.29	99.95
Cr	2300				2200			2943	2296	979	2095	853	3520	3667
Ni	1700				1600			985	1091	245	580	363	1417	1223
Co	120				100			83	73	68	83	80	83	92
V								179	140	189	206	80	87	92
Pb								12	6	6	8	11	6	13
Rb								2	2	2	2	2	2	2
Ba								97	84	124	113	118	8	98
Sr								16	16	25	20	10	62	22
Nb								6	4	3	4	7	3	5
Zr								24	24	25	30	36	13	31
Y								9	8	12	12	13	5	14

Table 1. (Contd.)

Com-ponent	90-1	90-2	350-61	9-50	15-1	15-2	8-1	829-1	844-1	847-1	849-1	51	52	54
SiO_2	40.60	47.49	46.38	49.70	51.06	44.64	50.32	51.20	52.98	51.88	49.82	50.82	53.60	52.50
TiO_2	0.99	0.83	0.38	0.39	0.26	0.45	0.76	0.60	0.55	0.75	0.59	0.93	0.63	0.59
Al_2O_3	15.64	13.48	11.28	9.96	4.99	9.18	13.36	13.39	12.65	14.42	14.02	10.42	12.71	13.25
Fe_2O_3	2.03	1.52	2.19	2.55	0.76	1.38	3.52	2.99	2.82	2.97	1.98	3.32	2.22	1.73
FeO	12.21	10.69	9.82	8.47	7.69	9.20	7.90	8.38	8.26	8.31	8.03	9.19	8.33	8.47
MnO	0.20	0.18	0.18	0.14	0.25	0.33	0.16	0.24	0.17	0.19	0.19	0.23	0.19	0.17
MgO	17.43	15.32	15.95	14.87	21.11	21.37	9.42	5.84	8.50	7.55	8.36	9.32	8.54	8.80
CaO	0.56	1.26	6.37	6.16	9.95	7.43	4.70	8.43	8.20	7.28	8.41	8.65	6.05	5.83
Na_2O	0.13	0.09	1.09	2.14	0.11	0.13	3.55	1.73	2.47	3.03	2.67	2.81	4.20	3.77
K_2O	0.01	0.01	0.08	0.09	0.01	0.01	0.04	0.03	0.09	0.14	0.23	0.70	0.63	0.15
P_2O_5			0.03						0.08			0.16	0.08	0.04
H_2O	0.30	0.18	0.22	0.16	0.08	0.25	0.13	0.11	0.10	0.15	0.22	0.41	0.29	0.12
LOI	9.57	8.78	5.98	5.11	3.38	5.38	5.68	6.70	3.44	3.45	5.31	3.12	2.49	4.16
Total	99.67	99.83	99.95	99.74	99.65	99.75	99.54	99.64	100.3	100.1	99.83	100.1	99.96	99.58
Cr	46	21	1200	915	2242	3063	469	171	292	76	213	594	242	160
Ni	110	82	260	151	1057	1295	98	66	107	53	81	257	75	63
Co	66	59	79	58	71	81	57	49	47	47	45	68	66	48
V	285	374		232	129	139	50	208	247	241	226	181	300	243
Pb	11	6		8	7	11	6	8	6	10	9	19	15	7
Rb	3	2		3	2	4	2	2	6	3	6	16	11	5
Ba	8	97		8	98	91	100	119	95	115	140	165	245	69
Sr	10	11		52	12	8	56	116	101	131	111	131	141	132
Nb	6	2		2	5	7	6	5	3	4	4	9	4	4
Zr	41	42		33	21	32	52	46	41	46	39	93	47	43
Y	13	13		16	9	10	19	17	19	20	14	19	20	21

Note: Komatiite: 40-51, 40-50, and 41-1—roof of a lava flow with polygonal parting; 95-1, 40-1, 350-8a, 350-1, 94-1, 2-1, 90-1, and 90-2–massive lava; 2-2—roof breccia; 2-3, 5480, 350-32, 350-64, 350-61, and 9-50—zone of spinifex textures in a lava flow; 15-1, 15-2, and 8-1—agglomerate komatiite tuff. Tholeiitic basalts: 829-1, 844-1, 847-1, and 849-1—massive lava. Gabbro: 51, 52, and 54.

Table 2. Composition (wt %, ppm) of rocks of the komatiite–tholeiite association from the Palasel'ga structure

Component	275-16	275-1a	275-2	275-6	275-9	275-51	5410-6	5411-1	5434-4	60-5	60-8a	60-8b	60-9	60-11
SiO_2	41.54	41.24	40.82	39.16	46.78	42.00	43.54	46.10	46.46	49.32	47.42	51.96	49.58	45.72
TiO_2	0.28	0.22	0.25	0.30	0.21	0.19	0.30	0.41	0.38	0.36	0.40	0.38	0.36	0.40
Al_2O_3	5.60	5.89	6.40	6.50	5.64	5.98	7.68	9.19	9.45	10.76	9.72	12.56	11.30	11.46
Fe_2O_3	3.51	5.35	4.36	5.75	4.83	1.88	6.06	1.84	1.89	3.59	1.62	1.96	1.59	2.27
FeO	6.56	6.32	6.25	7.04	5.89	9.52	6.03	10.20	9.46	8.38	11.50	8.86	10.54	11.76
MnO	0.11	0.13	0.13	0.14	0.11	0.13	0.11	0.20	0.26	0.16	0.23	0.14	0.18	0.19
MgO	30.03	28.62	29.14	29.05	26.65	29.80	24.12	18.09	17.89	9.60	14.32	9.30	12.25	13.50
CaO	2.47	3.36	3.36	3.08	3.64	3.18	6.16	8.96	8.90	14.14	9.17	9.04	8.27	8.68
Na_2O	0.06	0.01	0.03	0.02	0.11	0.05	0.25	0.50	0.79	1.17	1.48	3.25	2.27	1.68
K_2O	0.02	0.01	0.01	0.01	0.01	0.02	0.02	0.05	0.05	0.17	0.18	0.17	0.24	0.23
P_2O_5	0.13					0.01	0.01			0.02	0.04	0.04	0.04	0.04
H_2O	0.25	0.21	0.19	0.18	0.18	0.18	0.12	0.17	0.07	0.14	0.26	0.08	0.08	0.12
LOI	8.95	7.87	7.95	8.06	5.38	6.95	5.34	4.21	4.12	1.95	3.46	1.96	3.04	3.86
Total	99.51	99.23	99.89	99.29	99.43	99.89	99.74	99.92	99.72	99.76	99.80	99.70	99.74	99.91
Cr	4343	4154	5476	5026	4941	4233	4582	2567	3153	790	950	588	833	1082
Ni	1285	1408	1392	1387	1269	1635	964	598	1197	79	186	93	148	236
Co	105	115	104	126	99	75	72	77	76	45	62	50	64	69
V	131	128	124	107	101	107	119	167	110	204	191	230	187	208
Pb	12	13	15	13	8	18	13	8	10	6	13	7	8	8
Rb	2	2	3	2	4	4	2	4	2	8	9	211	13	9
Ba	8	97	116	8	8	15	19	114	80	120	130	128	99	126
Sr	6	7	8	4	6	8	9	18	8	217	35	126	62	39
Nb	3	7	2	5	2	0	2	4	3	4	4	4	7	5
Zr	16	15	21	16	5	9	15	23	19	27	26	31	26	28
Y	5	7	8	6	5	4	6	7	8	16	12	14	14	12

Table 2. (Contd.)

Com-ponent	5401-3	5401-1	5460-5	5468-1	5468-a	5492-1	5414-1	5415-1	5419-1	5421-4	16-1	16-3	17-8	5462-1
SiO_2	50.80	49.86	51.90	45.84	45.64	49.53	58.50	53.16	53.20	49.32	44.10	43.84	49.22	44.40
TiO_2	0.31	0.36	1.21	1.70	1.70	0.59	0.78	0.83	0.93	0.85	0.42	0.40	0.51	0.44
Al_2O_3	5.32	6.60	15.47	10.60	10.80	5.12	15.72	15.48	14.63	15.94	17.01	13.88	14.10	12.02
Fe_2O_3	2.88	3.36	1.35	5.22	5.29	1.05	1.34	2.02	2.28	1.19	2.12	1.49	1.97	1.30
FeO	8.18	7.75	8.50	10.78	10.54	8.54	5.99	8.26	6.58	10.18	8.62	11.35	8.04	13.05
MnO	0.32	0.30	0.14	0.17	0.17	0.19	0.14	0.19	0.19	0.24	0.13	0.16	0.14	0.16
MgO	19.51	19.33	5.85	8.70	8.65	20.05	4.52	5.13	6.14	6.66	12.39	15.06	10.88	12.90
CaO	10.08	9.80	5.47	11.18	11.66	10.39	5.88	10.53	11.09	10.64	7.15	7.43	7.08	8.66
Na_2O	0.35	0.55	4.25	2.00	1.81	0.25	3.97	2.22	3.17	2.94	1.23	1.23	1.48	1.31
K_2O	0.03	0.04	2.65	0.36	0.33	0.04	1.45	0.35	0.08	0.37	2.10	0.70	3.00	0.49
P_2O_5			0.47	0.00	0.00	0.00	0.24	0.00	0.00	0.00	0.00	0.00	0.00	0.00
H_2O	0.11	0.09	0.11	0.24	0.22	0.12	0.06	0.06	0.08	0.07	0.22	0.14	0.15	0.22
LOI	2.04	2.11	2.22	3.11	2.98	3.95	1.29	1.54	1.43	1.66	4.12	4.18	2.50	4.85
Total	99.93	100.2	99.59	99.91	99.79	99.82	99.88	99.77	99.80	100.1	99.61	99.86	99.07	99.80
Cr	1320	3100	115	186	184	1567	61	377	383	340	220	229	618	746
Ni	675	718	65	110	129	669	18	124	113	130	220	277	112	134
Co	68	70	61	55	51	61	55	59	44	55	42	53	36	48
V	148	158	223	284	297	105	172	312	324	325	84	109	122	166
Pb	9	15	13	18	20	23	19	11	11	8	10	12	15	11
Rb	2	2	16	11	7	2	56	18	2	19	69	25	106	12
Ba	99	8	101	150	107	80	383	143	109	152	764	10	1604	192
Sr	11	10	169	324	418	82	226	119	89	97	41	55	92	70
Nb	3	4	14	12	11	5	10	5	3	4	4	4	4	4
Zr	20	17	223	123	94	36	75	48	53	46	30	30	34	24
Y	10	10	32	34	29	10	26	18	20	22	6	9	8	11

Note: Komatiite: 275-16 and 275-1a—cumulative zone of a lava flow; 275-2, 275-6, 5411-1, 60-5, 60-8a, 60-8b, and 60-9—zone of spinifex textures in a lava flow; 275-9—roof breccia; 275-51 and 60-11—massive lava; 5410-6 and 5434-4—roof of a lava flow with polygonal parting; 5401-3 and 5401-1—agglomerate tuff. Tholeiitic basalts of the lower level: 5460-5—pillow lava; 5468-1, 5468-a, and 5492-1—massive lava. Tholeiitic basalts of the upper level: 5414-1 and 5415-1—massive lava; 5419-1 and 5421-4—pillow lava. Intrusive rocks: 16-1, 16-3, 17-8, and 5462-1—gabbro.

Table 3. Composition (wt %, ppm) of rocks of the komatiite–tholeiite association from the Sovdozero structure

Component	9m01	9m05-1	9m05-2	9m08-2	9m08-3	9m18-1	9m18-2	9m18-3	9m19-1	9m20	9m21	9m27	9m43	9m51
SiO_2	42.38	41.40	40.26	42.74	42.72	43.78	47.68	44.22	40.84	42.60	43.42	41.74	38.28	44.66
TiO_2	0.29	0.35	0.43	0.27	0.31	0.44	0.24	0.43	0.31	0.29	0.33	0.25	0.20	0.25
Al_2O_3	5.83	6.58	7.57	5.34	5.05	8.38	4.84	8.92	6.63	6.11	6.09	5.88	4.06	5.08
Fe_2O_3	2.35	5.02	5.67	4.81	4.61	2.90	2.93	1.42	3.98	2.82	2.90	1.30	2.42	2.32
FeO	6.89	7.18	7.32	6.47	6.47	10.34	5.82	10.06	7.76	6.82	6.75	7.47	5.74	7.61
MnO	0.10	0.14	0.14	0.14	0.14	0.22	0.12	0.23	0.10	0.10	0.11	0.12	0.12	0.05
MgO	30.66	26.81	26.40	27.01	27.72	20.06	24.49	20.87	27.50	28.12	27.32	26.11	34.00	29.33
CaO	3.22	5.60	4.78	5.89	5.61	7.99	6.27	6.80	4.35	4.77	5.19	5.75	2.52	1.26
Na_2O	0.31	0.09	0.08	0.05	0.04	0.55	0.11	0.30	0.05	0.06	0.06	0.05	0.03	0.02
K_2O	0.01	0.02	0.04	0.01	0.01	0.07	0.01	0.04	0.01	0.01	0.01	0.02	0.01	0.01
P_2O_5								0.07						
H_2O	0.15	0.31	0.06	0.08	0.30	0.32	0.20	0.16	0.22	0.26	0.20	0.12	0.12	0.02
LOI	7.63	6.24	7.06	6.89	6.92	4.87	4.90	6.15	8.04	7.76	7.18	10.83	12.51	9.28
Total	99.82	99.74	99.81	99.70	99.90	99.92	97.61	99.67	99.79	99.72	99.56	99.64	100.0	99.92
Cr	3303	4180	4443	3958	3148	2803	2580	3009	2854	2529	3070	2516	2181	5079
Ni	1481	1038	1020	1406	1258	574	822	502	1189	1290	1167	1521	1862	1319
Co	80	64	78	73	67	100	58	61	92	91	82	107	114	90
V	37	83	66	73	47	95	59	90	89	60	41	58	28	56
Pb	6	6	9	7	6	6	7	14	12	9	6	12	6	12
Rb	2	2	2	2	2	4	2	2	2	2	2	2	4	2
Ba	167	10	133	10	138	10	243	153	10	10	148	10	10	10
Sr	10	19	19	21	20	32	34	31	18	27	21	22	15	15
Nb	4	4	4	4	4	4	4	4	4	4	4	4	4	4
Zr	18	16	23	14	13	26	21	16	15	17	17	15	12	10
Y	6	8	7	10	8	4	6	11	8	8	5	7	7	5

Table 3. (Contd.)

Com-ponent	920	921	923	924	970	971	975	978	9m49	9m49b	9m52	9m56	9m55a	9m55b
SiO_2	48.94	47.64	49.84	48.96	49.90	48.62	50.94	50.04	53.70	51.52	51.30	40.20	41.30	31.26
TiO_2	0.86	0.84	0.89	0.80	1.15	1.78	0.63	0.57	0.65	0.83	0.58	0.13	0.51	1.14
Al_2O_3	14.67	13.59	13.36	14.42	14.93	11.42	14.93	15.97	12.40	13.30	14.79	2.53	9.61	16.54
Fe_2O_3	2.75	2.07	1.69	2.82	1.82	2.80	1.42	2.22	1.46	1.44	0.95	0.83	0.27	0.28
FeO	9.22	10.20	10.54	8.62	10.42	14.22	7.90	6.47	8.05	10.77	7.97	6.82	10.92	15.23
MnO	0.19	0.18	0.18	0.16	0.19	0.20	0.15	0.15	0.14	0.17	0.12	0.07	0.14	0.15
MgO	6.65	9.37	9.16	8.16	5.85	6.05	7.56	9.27	8.47	7.06	8.77	31.14	23.18	21.72
CaO	11.64	11.49	10.23	10.37	9.53	9.67	11.21	7.99	8.83	8.13	10.23	1.96	6.30	3.01
Na_2O	2.70	2.66	2.65	2.48	3.49	2.83	2.66	3.28	3.94	4.54	3.50	0.02	0.06	0.09
K_2O	0.24	0.24	0.44	0.22	0.35	0.34	0.33	1.39	0.40	0.65	0.22	0.01	0.01	0.05
P_2O_5	0.10		0.11	0.06	0.12		0.08	0.06						
H_2O	0.02	0.11	0.15	0.18	0.12	0.17	0.07	0.06	0.13	0.10	0.08	0.03	0.10	0.06
LOI	1.55	1.62	1.54	2.34	1.66	1.58	1.81	2.19	1.65	1.55	1.52	16.02	7.37	10.15
Total	99.53	100.1	100.8	99.59	99.53	99.68	99.69	99.66	99.82	100.1	100.0	99.76	99.77	99.68
Cr	261	284	262	288	200	57	261	728	82	39	116	1300	2441	9
Ni	92	85	80	998	65	12	128	145	67	39	62	1792	746	65
Co	49	35	57	48	50	45	30	43	41	42	38	76	58	71
V	185	213	177	177	147	483	147	122	122	152	101	24	74	192
Pb	9	6	6	6	6	6	12	21	6	9	6	6	6	6
Rb	2	3	28	2	7	10	8	93	9	15	3	2	2	2
Ba	10	10	10	10	10	10	10	10	10	149	152	177	10	10
Sr	122	127	60	96	132	71	147	145	146	84	216	15	10	9
Nb	4	4	4	4	8	4	4	4	4	4	5	4	4	6
Zr	44	55	54	40	71	53	43	33	40	48	38	11	32	71
Y	20	27	19	20	26	24	16	16	17	21	16	5	12	30

Note: Komatiite: 9m01, 9m05-1, 9m21, 9m43, and 9m51—massive lava; 9m05-2, 9m08-2, 9m08-3, 9m18-2, and 9m19-1—roof breccia; 9m18-1, 9m18-3, and 9m27—zone of spinifex textures in a lava flow; 9m20—roof of a lava flow with polygonal parting. Tholeiitic basalts of the lower level: 920, 923, and 924—massive lava; 921—pillow lava. Tholeiitic basalts of the upper level: 970 and 978—pillow lava; 971 and 975—massive lava. Intrusive rocks: 9m49, 9m49b, 9m52—gabbro; 9m56, 9m55a, and 9m55b—dunite.
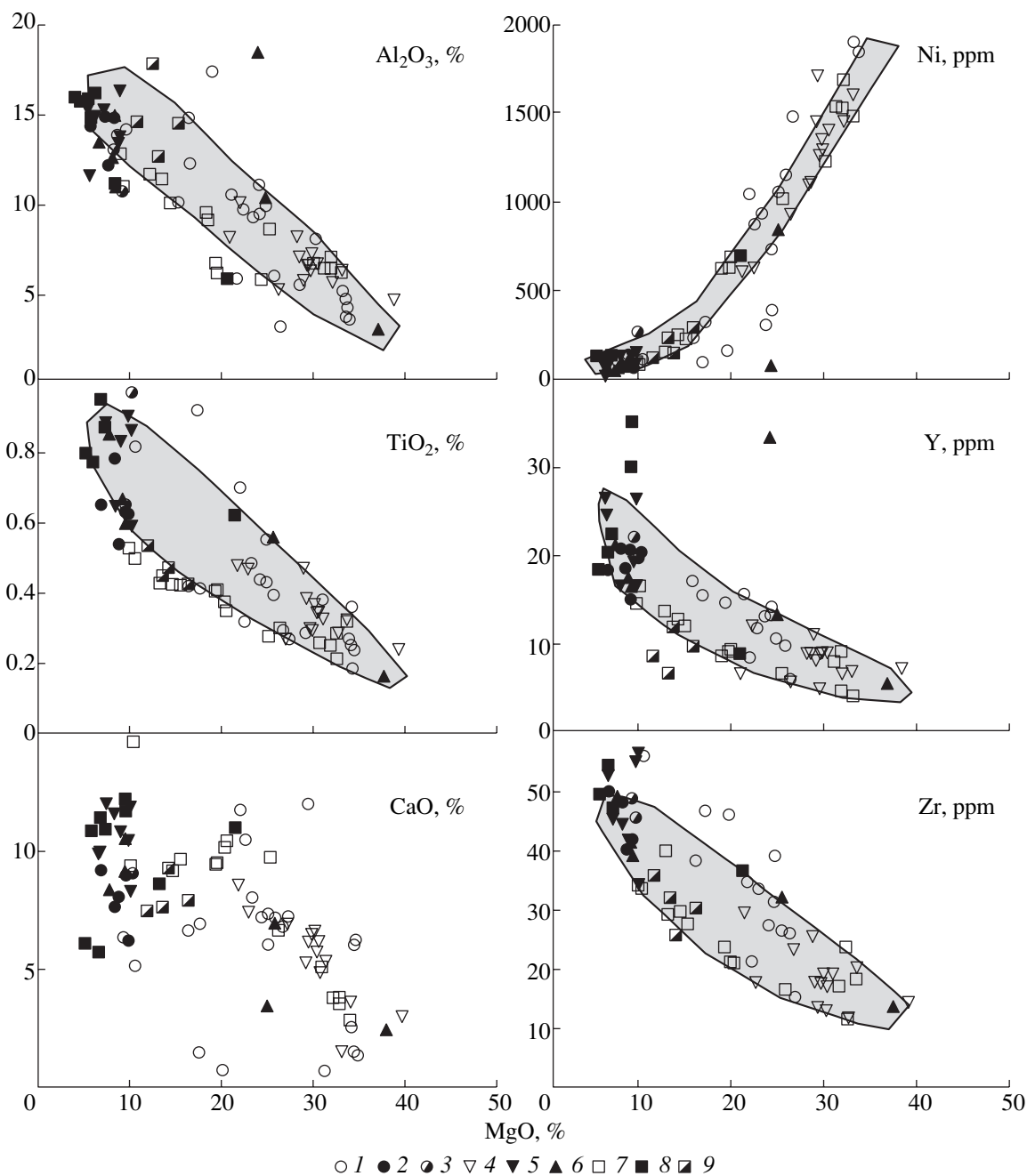
Fig. 3. MgO–Al$_2$O$_3$, –TiO$_2$, –CaO, –Ni, –Y, and –Zr plots for rocks of the komatiite–tholeiite association of the Vedlozero–Segozero greenstone belt.
Koikary structure: (*1*) komatiite, (*2*) tholeiitic basalt, (*3*) intrusive rocks; Sovdozero structure: (*4*) komatiite, (*5*) tholeiitic basalt, (*6*) intrusive rocks; Palasel'ga structure: (*7*) komatiite, (*8*) tholeiitic basalt, (*9*) intrusive rocks. Shaded field is the trend of the high-Mg volcanic rocks based on preexisting data.

unfractionated LREE patterns (Fig. 4a) and (La/Sm)$_n$ ratio in them is equal to 0.94 ± 0.41 (Gd/Yb)$_n$ = 1.16 ± 0.21, (Ce/Yb)$_n$ = 0.95 ± 0.23. Two samples of these rocks from the Sovdozero structure (Fig. 4c) have unfractionated LREE patterns and (La/Sm)$_n$ = 1.00 ± 0.08, (Ce/Yb)$_n$ = 0.89 ± 0.06; three samples are weakly depleted and have (La/Sm)$_n$ = 0.68 ± 0.22, (Ce/Yb)$_n$ =

0.58 ± 0.16; and two samples are enriched in LREE with (La/Sm)$_n$ = 2.28 ± 0.51, (Ce/Yb)$_n$ = 1.73 ± 0.66. All of the samples have similar (Gd/Yb)$_n$ values of 1.09 ± 0.13. It was determined that komatiites and some tholeiitic basalts from the Palasel'ga structure (Fig. 4b) are depleted in LREE: (La/Sm)$_n$ = 0.63 ± 0.20, (Gd/Yb)$_n$ = 0.99 ± 0.08, and (Ce/Yb)$_n$ = 0.61 ± 0.16, excluding two tholeiite samples, which are enriched in

Table 4. REE concentrations (ppm) in rocks of the tholeiite–komatiite association of the Vedlozero–Segozero greenstone belt

| Sample	La	Ce	Pr	Nd	Sm	Eu	Gd	Tb	Dy	Ho	Er	Tm	Yb	Lu
						Koikary structure								
41-1	0.45	1.52	0.30	1.76	0.69	0.26	1.13	0.19	1.17	0.27	0.80		0.66	0.12
9-50	0.96	2.60	0.45	2.58	1.01	0.42	1.43	0.26	1.89	0.41	1.08	0.17	1.18	0.16
2-1	0.51	2.18	0.32	1.83	0.66	0.40	1.17	0.23	1.62	0.32	0.89	0.17	0.99	0.15
90-1	2.42	5.70	0.60	2.42	0.79	0.34	1.34	0.26	1.95	0.43	1.37	0.21	1.52	0.22
350-61	1.59	4.81	0.57	2.45	0.79	0.31	1.31	0.23	1.59	0.33	1.01	0.14	0.94	0.14
8-1	2.03	5.66	0.96	5.34	2.03	0.64	3.20	0.49	2.99	0.68	1.92		1.71	0.28
847-1	2.80	6.81	1.07	4.56	1.43	0.76	2.03	0.38	2.63	0.59	1.64	0.24	1.69	0.23
849-1	2.47	5.78	0.86	4.36	1.51	0.48	2.03	0.34	2.29	0.47	1.46	0.21	1.31	0.21
						Palasel'ga structure								
275-16	0.24	0.82	0.14	0.86	0.41	0.06	0.60	0.09	0.71	0.16	0.43	0.07	0.49	
275-51	0.24	0.79	0.12	0.62	0.30	0.08	0.46	0.09	0.64	0.15	0.41	0.06	0.40	
5410-6	0.19	0.69	0.00	0.66	0.33	0.00	0.44	0.07	0.57	0.13	0.34	0.00	0.43	
60-5	2.62	5.04	0.75	3.72	1.22	0.52	1.78	0.30	1.95	0.42	1.28	0.20	1.29	0.22
60-8a	0.65	2.05	0.32	1.92	0.79	0.33	1.21	0.21	1.46	0.33	1.00	0.16	1.02	0.15
60-8b	1.08	3.21	0.44	2.75	1.05	0.37	1.56	0.26	1.95	0.37	1.19	0.19	1.14	0.20
60-9	0.68	1.98	0.32	2.00	0.73	0.28	1.14	0.21	1.42	0.32	1.05	0.16	1.02	0.17
60-11	0.70	1.97	0.37	1.85	0.80	0.30	1.26	0.22	1.69	0.35	1.11	0.18	1.15	0.18
5414-1	19.10	43.20	5.35	22.10	4.48	1.07	4.52	0.71	3.99	0.83	2.47	0.36	2.35	0.36
5460-5	17.80	44.40	5.92	24.50	5.34	1.33	5.75	0.90	5.44	1.06	3.03	0.45	3.00	0.42
						Sovdozero structure								
9m19-1	0.30	0.92	0.20	1.22	0.55	0.16	0.83	0.15	0.95	0.21	0.62	0.09	0.63	
9m03-3*	1.05	1.96	0.33	1.82	0.74	0.16	1.00	0.17	1.12	0.22	0.65	0.11	0.66	0.12
9m03-2*	0.37	1.01	0.23	0.92	0.31	0.06	0.73	0.11	0.73	0.17	0.44	0.08	0.55	
9m18-3	3.41	7.84	0.78	3.35	0.79	0.30	1.44	0.21	1.71	0.34	0.91	0.13	0.91	0.11
9m01	1.45	2.32	0.35	1.53	0.53	0.18	0.54	0.10	0.86	0.18	0.53	0.10	0.60	0.10
9m05-2	1.20	2.30	0.40	1.80	0.72	0.21	0.79	0.14	1.20	0.26	0.74	0.12	0.67	0.11
9m08-3	1.30	2.60	0.40	1.90	0.71	0.24	0.83	0.15	1.05	0.22	0.67	0.11	0.59	0.10

* Roof breccia of peridotitic komatiite.

LREE: $(La/Sm)_n = 2.45 \pm 0.30$, $(Gd/Yb)_n = 1.59 \pm 0.02$, and $(Ce/Yb)_n = 4.61 \pm 0.49$ at elevated concentrations of SiO_2, Y, Zr, Nb, Sr, Ba, and Rb. The REE distribution is topologically similar in the rocks of various zones (spinifex, cumulate, and roof breccia) within lava flows, between the chill zones of pillow lavas and the cores of pillows (Koikary and Palasel'ga structures).

Sm–Nd ISOTOPIC DATA

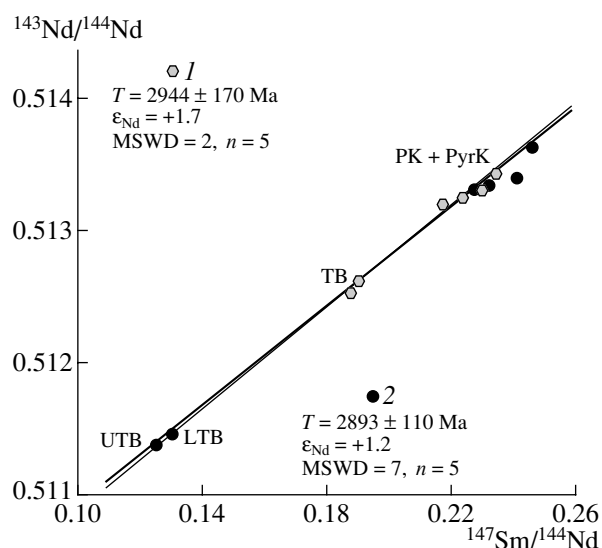Table 5 summarizes Sm–Nd data on the rocks. The primary ε_{Nd} values for all rocks were calculated with the use of the model age of 2940 Ma. Among rocks from the Palasel'ga stricture, we analyzed komatiites and tholeiitic basalts strongly enriched in LREE. Except for one sample (275-16), all of the komatiites have positive ε_{Nd} values. The negative ε_{Nd} can be explained be REE migration during overprinted Proterozoic metamorphism, as was also proposed for komatiites in eastern Finland [20]. In the analyzed sampling of volcanic rocks from the Koikary structure with calculated $\varepsilon_{Nd} = +1.7$ (2940 Ma), one sample (90-1) has an ε_{Nd} significantly shifted toward positive values (it equals +4.7). The Koikary and Palasel'ga tholeiitic
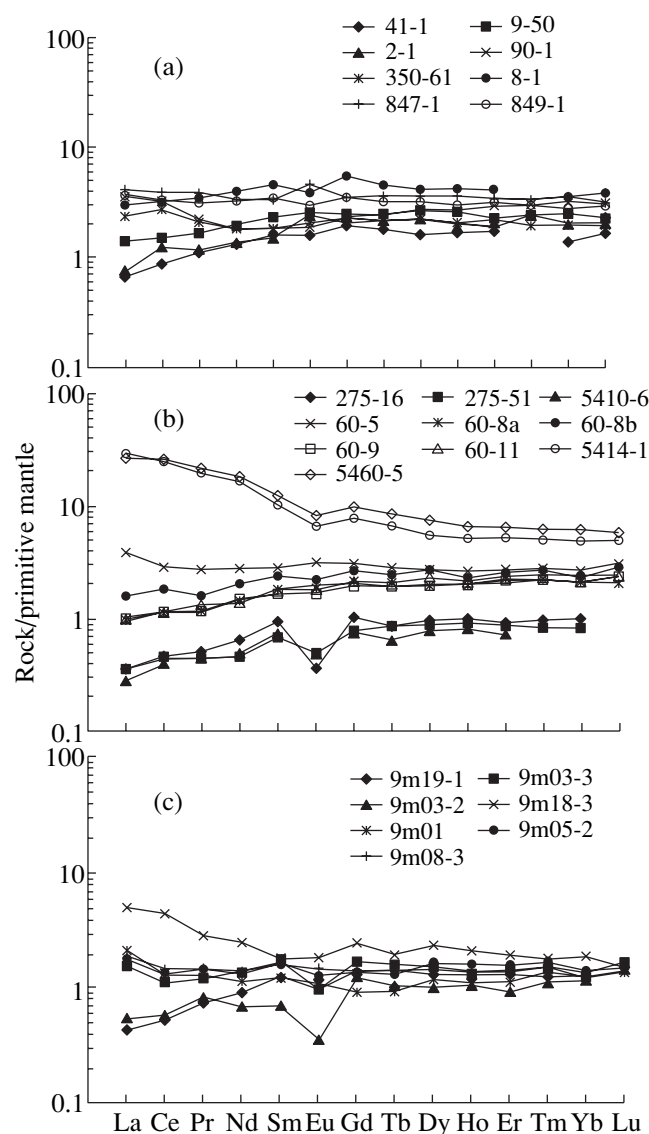
Fig. 4. REE patterns (normalized to the primitive mantle [19]) for rocks the komatiite–tholeiite association in (a) the Koikary, (b) Palasel'ga, and (c) Sovdozero structures.

See notes to Tables 1, 2, and 3 for rock descriptions.

Fig. 5. Sm–Nd diagram for rocks the komatiite–tholeiite association in (*1*) the Koikary, (*2*) Palasel'ga.

PK + PyrK—peridotitic and pyroxenitic komatiites, TB—tholeiitic basalts (Koikary structure), UTB—tholeiitic basalts of the upper level, LTB—tholeiitic basalts of the lower level (Palasel'ga structure).

basalts (with chondritic LREE patterns and LREE-enriched, respectively) have similar ε_{Nd} from +1.2 to +1.8 (Table 5, Fig. 5).

The Sm–Nd age of the komatiite–tholeiite association of the Palasel'ga structure (calculated based on five samples, except Sample 275-16) is 2893 ± 110 Ma, ε_{Nd} = +1.2, MSWD = 7. The analogous values for volcanics from the Koikary structure (calculated based on five samples, except Sample 90-1) are 2944 ± 170 Ma, ε_{Nd} = +1.7, MSWD = 2 (Fig. 5). The computations were carried out under the assumption that the basaltic and komatiitic lavas are coeval. Stratigraphic data on reference cross sections within the Vedlozero–Segozero greenstone belt provide evidence that the komatiite–tholeiite association belongs to a single stratigraphic

level, which can be used as a marker in partial sections within the belt [4, 9, 14]. Based on these data, the age of the komatiite–tholeiite association in the Vedlozero–Segozero greenstone belt can be assayed using ten samples of volcanic rocks from both structures (excluding samples with anomalous ε_{Nd} values). In this case, the Sm–Nd age equals 2921 ± 55 Ma, ε_{Nd} = +1.5, MSWD = 5. These data are in good agreement with the zircon age of crosscutting dacite dikes in the Koikary structure (2860 ± 15 Ma [12] and 2935 ± 20 Ma [11]).

MAGMA GENERATION CONDITIONS

The komatiites of the Vedlozero–Segozero greenstone belt affiliate with the Al-undepleted type, and this implies that the rocks were produced at high partial melting degrees (>40%) and pressures of approximately 6 GPa, with the predominance of olivine at the liquidus [21–24]. Our data make it possible to calculate the *P–T* conditions of magma generation and eruption of komatiitic magmas within the examined geologic structures.

In order to determine the temperatures of the komatiitic melt during its surface eruption ($T°C_{liq}$), we used an experimentally derived equation for the dependence of the Mg# of melt on temperature [25]. The $T°C_{liq}$ values were then converted to the potential (maximum possible) temperature of magma generation ($T°C_{pot}$) by an equation from [23]. The pressure in the mantle source was assayed based on the Al_2O_3 concentration in the primary melt expressed as a function of temperature [24]. The accuracy of the liquidus temper-

Table 5. Sm–Nd isotopic data on komatiite–tholeiite associations of the Koikary and Palasel'ga structures

Sample	Rock	Sm (ppm)	Nd (ppm)	$^{147}Sm/^{144}Nd$	$^{143}Nd/^{144}Nd$	2δ	ε_{Nd} (2940)
	Komatiite–tholeiite association of the Koikary structure						
9-50	Pyroxenitic komatiite	1.15	3.04	0.2291	0.513343	10	+1.4
350-61	Pyroxenitic komatiite	0.87	2.33	0.2243	0.513256	13	+1.5
90-1	Pyroxenitic komatiite	0.83	2.30	0.2176	0.513288	12	+4.7
2-1	Pyroxenitic komatiite	0.78	2.02	0.2322	0.513424	22	+1.8
847-1	Tholeiitic basalt	1.37	4.35	0.1898	0.512573	11	+1.3
849-1	Tholeiitic basalt	1.64	5.20	0.1910	0.512624	10	+1.8
	Komatiite–tholeiite association of the Palasel'ga structure						
5410-6	Peridotitic komatiite	0.30	0.75	0.2449	0.513603	21	+0.5
275-16	Peridotitic komatiite	0.38	0.95	0.2414	0.513395	15	–2.3
60-8a	Pyroxenitic komatiite	0.82	2.18	0.2268	0.513297	13	+1.4
60-9	Pyroxenitic komatiite	0.83	2.16	0.2319	0.513340	20	+0.3
5460-5	Tholeiitic basalt of the lower level	5.97	27.87	0.1295	0.511430	10	+1.8
5414-1	Tholeiitic basalt of the upper level	5.04	24.25	0.1256	0.511321	10	+1.2

Note: The $^{147}Sm/^{144}Nd$ ratio was measured accurate to 0.4%. The $^{143}Nd/^{144}Nd$ ratio was normalized to $^{146}Nd/^{144}Nd = 0.7219$. The measured value of the La Jolla standard was $^{143}Nd/^{144}Nd = 0.511851 \pm 6$ ($n = 15$).

ature calculation (calculated with allowance for the analytical errors of the XRF technique) was ±13°C, that for the magma generation temperature was ±18°C, and the pressure was assayed accurate to ±0.4 GPa. The parameters of komatiitic magma generation were evaluated with the use of the compositions of chill zones in lava flows, with all *P–T* estimates considered to be the maximum possible.

Our calculations led us to formulate the following conclusions. The maximum eruption temperatures of the peridotitic komatiites did not exceed 1600°C (<1556°C for Koikary, <1567°C for Palasel'ga, and <1588°C for Sovdozero). The magma generation temperatures lay within the range of 1781–1817°C (<1781°C for Koikary, <1794°C for Palasel'ga, and <1817°C for Sovdozero), which is 220–280°C higher (on the average) than the Archean mantle temperature at 2.9–3.1 Ga [26] at pressures no higher than 7.3 GPa (<7.29 GPa for Koikary, <6.93 GPa for Palasel'ga, and <6.42 GPa for Sovdozero). The magma was generated at depths of 210–240 km. The 45–60% partial melting took place during the ascent of a mantle plume in the course of adiabatic decompression, and this process produced harzburgite (*Ol + Opx*) residue. This is correlated with the genesis of the Munro komatiites, as was described by Herzberg [24]. The weakly depleted LREE distribution (which is most typical of the komatiites) seems to have been a consequence of certain features of the source. The derivation of magmas enriched in LREE should be related to the crustal contamination of the primary magmas during their ascent to the surface.

Based on experimental data [7, 21, 22, 27], we determined the crystallization sequence of the komati-

itic magmas. In our case, it can be hypothesized that, after their eruption at the surface at temperatures of approximately 1400°C, magnesian olivine started to crystallize in the melt. Later, the magnesian olivine was joined by ferrous olivine and, starting from 1250°C, by spinel. Hence, there was a wide temperature interval over which the primary magma evolved under olivine control. The fractionation and accumulation of this mineral resulted in an association of rocks from peridotitic to basaltic komatiites.

The high-Mg tholeiitic basalts could be produced by the differentiation of komatiitic melts or be derived from shallower sources. The genesis of these rocks remains not fully clear as of yet.

CONCLUSIONS

(1) Our geochemical investigations demonstrate that the komatiites of the Koikary, Palasel'ga, and Sovdozero structures in the Vedlozero–Segozero greenstone belt affiliate with Al-undepleted Munro type. The rocks resulted from 45–60% partial melting of a mantle source with harzburgite residue ($T < 1817°C, P < 7.3$ GPa) at depths of <240 km.

(2) The Sm–Nd system indicates that the komatiite–tholeiite association of the greenstone belt was generated at 2921 ± 55 Ma, ε_{Nd} = +1.5, MSWD = 5.

REFERENCES

1. Jahn, B.-M., Auvras, B., Blais, S., *et al.*, Trace Element Geochemistry and Petrogenesis of Finish Greenstone Belts, *J. Petrol.* 1980, vol. 21, pp. 201–244.

2. *Geological Development, Gold Mineralization and Exploration Methods in the Late Archean Hattu Schist Belt, Eastern Finland*, Nurmi, P.A. and Sorjonen-Ward, P., Eds., *Geol. Surv. Finland, Spec. Paper*, 1993, vol. 17.

3. *Komatiity i vesokomagnezial'nye vulkanity rannego dokembriya Baltiiskogo shchita* (Komatiites and High-Mg Volcanic Rocks of the Baltic Shield), Kulikov, V.S., Kulikova, V.V., *et al.*, Eds., Leningrad: Nauka, 1988.

4. *Stratigrafiya dokembriya Karelii. Opornye razrezy verkhnearkheiskikh otlozhenii* (Precambrian Stratigraphy of Karelia: Reference Cross Sections of Upper Archean Deposits), Rybakov, S.I., Ed., Petrozavodsk: Kol'skii Nauch. Tsentr Russ. Akad. Nauk, 1992.

5. Puchtel, I.S., Hofmann, A.W., Mezger, K., *et al.*, Oceanic Plateau Model of Continental Crustal Growth in the Archean: A Case Study from the Kostomuksha Greenstone Belt, NW Baltic Shield, *Earth Planet. Sci. Lett.,* 1998, vol. 155, pp. 57–74.

6. Vrevskii, A.B., *Petrologiya i geodinamicheskie rezhimy razvitiya arkheiskoi litosfery* (Petrology and Geodynamic Environments in the Evolution of the Archean Lithosphere), Leningrad: Nauka, 1989.

7. Smolkin, V.F., *Komatiitovyi i pikritovyi magmatizm rannego dokembriya Baltiiskogo shchita* (Komatiite and Picrite Magmatism in the Early Precambrian of the Baltic Shield), St. Petersburg: Nauka, 1992.

8. *Vulkanizm arkheiskikh zelenokamennykh poyasov Karelii* (Volcanism in the Archean Greenstone Belts of Karelia), Sokolov, V.A., Ed., Leningrad: Nauka, 1981.

9. Svetova, A.I., *Arkheiskii vulkanizm Vedlozersko–Segozerskogo zelenokamennogo poyasa Karelii* (Archean Volcanism in the Vedlozero–Segozero Greenstone Belt of Karelia), Petrozavodsk: Kol'skii Nauch. Tsentr Russ. Akad. Nauk, 1988.

10. Lobikov, A.F., On the Age of Early Karelian Volcanics: Lead Isochron Data, in *Problemy izotopnogo datirovaniya protsessov vulkanizma i osadkoobrazovaniya* (Problems of the Isotopic Dating of Volcanism and Sedimentation Processes), Kiev, 1982, pp. 90–91.

11. Bibikova, E.V. and Krylov, I.N., Isotopic Age of Acid Volcanics from Karelia, *Dokl. Akad. Nauk SSSR*, 1983, vol. 268, no. 5, pp. 1231–1235.

12. Samsonov, A.B., Bibikova, E.V., Puchtel, I.S., *et al.*, Isotopic and Geochemical Differences between Acid Volcanic Rocks from Greenstone Belts of Karelia and Their Geotectonic Significance, *Korrelyatsiya geologicheskikh kompleksov Fennoskandii* (Correlation between Geologic Complexes of Fennoscandia), St. Petersburg, 1996, p. 74.

13. Volodichev, O.I., Amphibole As an Indicator of Metamorphic Conditions of the Lopian Greenstone Rocks in Central and Western Karelia, in *Mineralogiya magmaticheskikh i metamorficheskikh porod dokembriya Karelii* (Mineralogy of Magmatic and Metamorphic Rocks in the Precambrian of Karelia), Petrozavodsk: Kol'skii Nauch. Tsentr Russ. Akad. Nauk, 1994, pp. 105–120.

14. Svetov, S.A., *Komatiit–toleitovye assotsiatsii Vedlozersko–Segozerskogo zelenokamennogo poyasa Tsentral'noi Karelii* (Komatiite–Tholeiite Associations of the Vedlozero–Segozero Greenstone Belt in Central Karelia), Petrozavodsk: Kol'skii Nauch. Tsentr Russ. Akad. Nauk, 1997.

15. Peltonen, P., Kontinen, A., *et al.*, Petrology and Geochemistry of Metabasalts from the 1.95 Ga Jormua Ophiolite, Northern Finland, *J. Petrol.* 1996, vol. 37, no. 6, pp. 1359–1383.

16. Jensen, L.S., A New Caption Plot for Classifying Subalkalic Volcanic Rocks, *Ontario Division of Mines*, 1976, MP66.

17. Arndt, N.T. and Lesher, C.M., Fractionation of REE by Olivine and Origin of Kambalga Komatiites, Western Australia, *Geochim. Cosmochim. Acta*, 1992, vol. 56, pp. 4191–4204.

18. Roeder, P.L. and Emslie, R.F., Olivine–Liquid Equilibrium, *Contrib. Mineral. Petrol.*, 1969, vol. 29, pp. 275–282.

19. Sun, S.S. and McDonough, W.F., Chemical and Isotopic Systematics of Oceanic Basalts: Implications for Mantle Composition and Processes, *Magmatism in Ocean Basins., Geol. Soc. Spec. Publ. 42,* Saunders, A.D. and Norry, M.J., Eds., no. 42, pp. 313–345.

20. Gruau, G., Tourpin, S., Forcade, S., *et al.*, Loss of Isotopic (Nd, O) and Chemical (REE) Memory during Metamorphism of Komatiites: New Evidence from Eastern Finland, *Contrib. Mineral. Petrol.*, 1992, vol. 112, pp. 66–82.

21. Girnis, A.V., Ryabchikov, I.D., and Bogatikov, O.A., *Genezis komatiitov i komatiitovykh bazal'tov* (Genesis of Komatiites and Komatiitic Basalts), Moscow: Nauka, 1987.

22. Girnis, A.V., Phase Equilibria in the Mantle with Reference to the Problem of the Genesis of High-Mg Magmas, *Doctoral (Geol.–Mineral.) Dissertation*, Moscow: Inst. Geol. Ore Deposits, Petrograph., Mineral., Geochem., Russ. Acad. Sci., 1998.

23. McKenzi, D.P. and Bickle, M.J., The Volume and Composition of Melt Generated by Extension of the Lithosphere, *J. Petrol.*, 1988, vol. 29, pp. 625–679.

24. Herzberg, C., Generation of Plume Magmas through Time: An Experimental Perspective, *Chem. Geol.*, 1995, vol. 126, pp. 1–16.

25. Renner, R., Cooling and Crystallization of Komatiite Flows from Zimbabwe, *PhD Thes.*, Cambridge, 1989.

26. Richter, F.M., A Major Change in the Thermal State of the Earth at the Archean–Proterozoic Boundary: Consequences for the Nature and Preservation of the Continental Lithosphere, *J. Petrol.*, 1988, spec. issue, pp. 39–52.

27. Zhang, J. and Herzberg, C., Melting Experiments on Anhydrous Peridotite KLB-1 from 5.0 to 22.5 GPa, *J. Geophys. Res.*, 1994, vol. 99, pp. 17 729–17 741.